Cefaly Dual Final Report

I. Introduction

Migraines are listed by the American Migraine Foundation as the third most common disease, and among the top ten most disabling medical illnesses in the world.[1] Cefaly Dual is a transcutaneous trigeminal nerve stimulator marketed as an over-the-counter (OTC) acute and preventative migraine treatment option. It was approved as a Class II OTC device by the FDA in 2020 via the 510(k) clearance process.[2] The device consists of a bipolar, self-adhesive electrode and a pulse generator that magnetically attaches to the electrode which allows for user-controlled stimulation amplitude. Cefaly claims the Cefaly Dual treats migraines through stimulation of the trigeminal nerve, reportedly via "segmental 'gate control' mechanisms."[3] Gate control theory asserts that activation of non-nociceptive sensory neurons engages inhibitory interneurons in the dorsal horn, thus closing the "gate" for transmission of painful, nociceptive signals.[4] Aß fibers are larger diameter, sensory neurons that transmit non-nociceptive signals, which in theory "block" nociceptive signals from smaller diameter A∂ fibers.

The Cefaly clinical trial was a double-blind, randomized, sham-controlled study of 106 patients with the primary outcome measure being the mean change in pain intensity at 1 hour compared to baseline, which is the duration of the acute treatment. The study reported a 59% decrease in the primary measure in the verum group compared to a 30% decrease in the sham group. However, a less significant reported pain decrease was seen at 24 hours compared to baseline, with a 57% decrease seen in the verum group compared to a 40% decrease in the sham group. An additional outcome measure reported by Cefaly was 79% pain relief and 32% total pain freedom during the trial. However, both verum and sham devices used "identical rectangular biphasic symmetrical pulses of 250 μs width that induced paresthesia," only differing

in frequency. NEURON does not allow for input of a frequency parameter; therefore, the difference between the verum and sham protocols could not be modeled. No serious adverse events were recorded, but some minor adverse events were recorded including paresthesia intolerance, drowsiness, and nausea. The main other inherent risk of the device is unintended nerve stimulation.

A series of computational studies by Salkim et al. analyzing the Cefaly device cited that 50% of a large population of Cefaly users were not satisfied with their results. They attributed this dissatisfaction to neuroanatomical differences in the targeted trigeminal nerve branches, specifically the supraorbital nerve (SON) and supratrochlear nerve (STN).[5, 6] They modeled the Cefaly device to determine if different locations of the SON resulted in significant current threshold differences and therefore differences in percent fiber activation. Using the McIntyre-Richardson-Grill (MRG) model and modeling 4 SON trajectories and 1 STN trajectory, they found a current range of 6 mA to 26 mA was required to activate all Aß fibers in all variations. This far exceeds the maximum Cefaly current of 16 mA, indicating these neuroanatomical variations could be the cause of inefficacy in some users.

Salkim et al. only analyzed Aß fiber activation and arbitrarily equated treatment efficacy with 50% fiber activation, not considering the effects of A∂ fiber activation on the proposed gate control mechanism. Our model aims to analyze the efficacy of the Cefaly device by investigating the impact of neuroanatomical variations on both Aß and A∂ fiber activation in four SON variations and one branched STN variation. Considering the biophysical model analysis as well as market analysis of the Cefaly device, this report provides a recommendation to Johnson & Johnson concerning the potential acquisition of Cefaly Dual.

II. Methods

To gain insight into the underlying mechanisms of action of the Cefaly device, we developed a computational biophysical model in NEURON implementing the McIntyre-Richardson-Grill double-cable myelinated axon model (***Figure 1***). This model has been validated for the modeling of myelinated, peripheral axons in mammals for fiber diameters within the Aß fiber range, ranging from 5.7 µm to 16 µm.[7] Our model only investigates the excitability of Aß fiber diameters within the range of axon diameters found in the ophthalmic nerve, the root of the SON and STN, which is 5.7 µm to 15 µm (***Figure 2***). To model smaller diameter A∂ fibers, we interpolated fiber geometrical parameters using equations acquired from Dr. Edgar Peña of the Grill Lab (***Equation 1***). It is important to note this method has not yet been extensively validated experimentally, yet we believe it to be a sufficient approximation of A∂ fiber geometry and suitable for our analysis. Although a therapeutically effective ratio of activation hasn't been identified, it is believed that sufficient activation of A∂ fibers could lead to enough pain signal transmission that causes the "pain gate" to open and cause an individual to still feel pain.[8]

Our model implements the Cefaly electrode geometry as two point-current sources separated by an interelectrode spacing of 13 mm centered on the midline of the forehead.[3] We derived the four SON locations and one STN location from data collected from two cadaveric studies (***Figures 3 and 4***). These four SON groupings exemplify average anatomical differences between individuals.[9, 10] The STN was modeled as two separate branches, a lateral (STN-L) and a medial (STN-M) branch, to ensure proper investigation of A∂ fiber activation due to the close proximity of this nerve to the midline. We assumed all nerves to have vertical trajectories and calculated the exact electrode to fiber distances relative to each nerve's protrusion through the frontalis muscle into the subcutaneous layer. This allowed us to more accurately model a homogeneous extracellular medium with a constant resistivity value of 0.00043 S/mm for skin.[6]

The Cefaly Dual stimulation parameters of a biphasic pulse with pulse width 250 µs were used to investigate fiber activation (***Figure 5***). The current threshold amplitude was found for each fiber diameter in each nerve, but the maximum Cefaly current amplitude of 16 mA was considered for analysis of the model results. We calculated percent activation of fibers to determine the overall ratio of Aß to A∂ fiber activation. We assumed the same Gaussian distribution of Aß fibers as Salkim et al. with a mean of 11.5 µm and standard deviation of 1.9 µm.[6] We used the histometric analysis density plot shown in ***Figure 2*** to assume a Gaussian distribution of A∂ fibers with a mean of 3.5 µm and standard deviation of 0.75 µm. For simplicity, we also assumed an equal distribution of fiber types between the STN and SON.

III. Results and Modeling Analysis

We first assessed the relationship between fiber diameter, electrode-to-fiber distance and activation threshold for the representative range of diameters of Aß fibers: 5.7 µm – 15 µm. ***Figure 6*** and ***Table 1*** show the activation thresholds across this range of Aß fiber diameters for STN-M and STN-L. Both branches exhibit activation thresholds that are inversely proportional to the square root of the fiber diameter, as expected from prior literature.[7] As the fiber diameter increases, the surface area of the membrane increases such that more current can move across the membrane. Larger diameter axons have larger internodal spacing which creates larger transmembrane voltage changes than fibers with smaller internodal spacing.

The STN-M branch exhibits a less pronounced inverse exponential decline in thresholds with respect to diameter because it is closer to the electrodes; current thresholds also depend on the distance between the stimulating electrodes and the nerve fiber. Transmembrane potentials created by extracellular current sources are largest in the fibers closer to the stimulating electrodes. Threshold current is known to be proportional to the square of the electrode-to-fiber

distance, which we also observe in our results.[7] The activation thresholds are on average three times higher for the STN-L compared to the STN-M; this can be explained by the STN-M being much closer to the midline of the forehead, where the electrodes would be placed on the user. Current-distance effects are observed to be stronger than current-diameter effects, so it is intuitive that fiber diameter has less of an effect on current threshold for the STN-M branch as these effects are overpowered by a small electrode-to-fiber distance. Additionally, all fiber diameters within this range are activated at thresholds within the working range of the Cefaly Dual device. The highest threshold was found to be 10.5 mA for the 5.7 μm fibers in the STN-L. As this current is lower than 16 mA, we can conclude that 100% of Aß fibers in the STN-M and STN-L would be activated using a current amplitude within the Cefaly Dual range.

We then investigated the current-diameter and current-distance relationships for four different trajectories of the SON nerve. These four groups varied in horizontal distance from the midline of the forehead, with SON1 as the closest to the midline and SON4 as the furthest, as shown in ***Table 2***.[6] ***Figure 7*** and ***Table 3*** show the activation thresholds across the same range of Aß fiber diameters for SON groups; SON variations exhibit even more pronounced inverse exponential relationships between current thresholds and fiber diameters as they are much farther from the electrodes than the STN branches. The largest range of threshold currents across diameters in the SON trajectories is 15 mA on average compared to 5.1 mA in the STN branches. Current-diameter effects thus become much more prominent at larger distances away from the electrodes. To further bolster this conclusion, the difference in threshold currents across the SON trajectories is minimal. The highest average difference in threshold currents is 0.42 mA, between SON2 and SON3. The salient difference in this analysis is the effect of a larger electrode-to-fiber distance on current thresholds between the STN and SON. In contrast to 100%

of STN branch nerve fiber activation below 16 mA, the average percent activation of fibers across the SON placements was 82.12%. Thus, a significant amount of smaller diameter Aß fibers will not be activated using the highest current parameter available to Cefaly Dual users.

Next, we performed the same analysis for the representative range of diameters of A∂ fibers: 1 µm – 5 µm. ***Figure 8*** and ***Table 4*** show the activation thresholds across this range of A∂ fiber diameters for the STN-M and STN-L branches. We observed similar inverse exponential relationships between fiber diameter and current thresholds to those found in Aß fibers for the STN branches. The STN-M also shows a less pronounced inverse exponential relationship to that of the STN-L, in a parallel fashion to our observations of Aß fibers. The key difference between Aß and A∂ fibers in the STN branches is the level of activation compared to the 16 mA current limit. While 100% of A∂ fibers in the STN-M branch are activated below 16 mA, only 20.23% of A∂ fibers in the STN-L are activated. Most A∂ fibers in the further STN-L branch require much greater currents to reach threshold than the larger Aß fibers. Thus, 100% of both the unintended nociceptive A∂ fibers are activated in addition to the targeted non-nociceptive Aß fibers in the STN-M branch. Although a much smaller fraction of A∂ fibers are activated in the STN-L branch in comparison to Aß fibers at the max current limit, these activations are still worrisome for the effectiveness of the proposed gate control mechanism for treating migraine as well as for pain at the site of stimulation. We found 0% activation of A delta fibers in all SON groupings for 16 mA and below, so we have chosen not to plot their thresholds as they are not relevant to the analysis of this device.

Our final analysis consisted in calculating percent fiber activations with respect to stimulus current level for each fiber type in each branch. We then calculated ratios of Aß fiber activation to A∂ fiber activation at different current levels. ***Figure 9*** shows the percent fiber

activation for Aß fibers as a function of stimulus current level. Both STN branches show steep activation curves as responses to small increases in stimulus current and saturate quickly. STN-M is activated first and saturates the fastest as it is the closest to the electrode. Although shifted to higher thresholds, STN-L activates at a similar rate for the first 6 points, then it saturates at a slightly lower rate as it is further from the electrodes than STN-M. The four SON groups also have much higher current thresholds and take higher currents to saturate as they are much further from the stimulating electrodes than the STN branches. We can clearly see from this plot that Aß fiber activation is much more affected by electrode-to-fiber distance than fiber diameter differences in this range. Our results are in line with the trends in fiber activation for each nerve branch as shown in the results from Salkim et al.

Figure 10 shows the percent activation versus stimulus current of A∂ fibers in the STN-M and STN-L branches. There is a clear tradeoff between activation of Aß fibers and A∂ fibers as the stimulus current increases. As shown in ***Table 5***, we calculated percent fiber activations for both fiber types for the maximum current setting on the device, 16 mA, as well as what we determined as a more optimal current setting, 14.4 mA. This current level was chosen to maximize the amount of Aß fiber activation while minimizing the amount of A∂ fiber activation according to our percent activation plots in Figures 8 and 9. As shown in ***Table 6***, we calculated the ratio of Aß fiber activation to A∂ activation using 16 mA stimulus current for each combination of STN branches with an SON grouping. We then calculated the activation ratios using 14.4 mA for each combination of STN branches with an SON grouping. The highest activation ratio using 16 mA is 2.44, compared to the highest activation ratio of 2.79 using 14.4 mA. Prolonged stimulation can result in Aß fiber adaptation such that A∂ fiber activation has an increased relative effect.[8] Thus, we can assume that the overall therapeutic effect would decrease

over the course of the 60-minute treatment. These ratios don't provide indisputable evidence for gate control theory and suggest pain at the site of stimulation. We also found that the current level to activate 0% total A∂ fibers total, 3.8 mA, would not activate any Aß fibers within SON trajectories, STN-L, and 100% of the Aß fibers in the STN-M. This current setting would only activate 33.3% of total Aß fibers in all branches we've considered, which we do not believe is therapeutically reasonable.

IV. Market Analysis

Migraines are the most common type of headaches, affecting 1 billion people worldwide. Mild migraines can be treated by OTC pain relievers, such as aspirin, acetaminophen or ibuprofen. However, when these do not work, other medications such as triptans, lasmiditan, CGRP antagonists, and ergots can be prescribed. Neuromodulation is often the next treatment option for people who do not experience relief from, or prefer to avoid, pharmaceutical drugs.[11] The market size for neuromodulation devices for the treatment of migraines is expected to grow from approximately $38 million in 2022 to $46 million by 2026, which makes it very desirable to acquire companies already on the market.[12] Within this market, there are four main devices that lead the field: Cefaly, Nerivio, GammaCore and Relivion MG.

Nerivio by Theranica is a transcutaneous electrical stimulator used to treat migraines by targeting sensory nerves of the upper arm. There are no reports on significant side effects, and it was first approved in 2019 for patients over 18 years old and in 2021 for patients over 12 years old.[13] However, this device can only be purchased with a prescription from a doctor, and it costs $599 for 12 treatments, after which a new device has to be purchased.[14] GammaCore is a vagus nerve stimulator approved by the FDA in 2018 that is intended to provide therapy by holding the device against the neck. Like Nerivio, this device can be used for patients age 12 and older, and

it can only be purchased if prescribed by a doctor. The price of the device is $598 per month, although some insurances cover the cost. Some of the side effects of this device are reaction at the application site, musculoskeletal disorders, metallic taste, dysgenisia and dizziness, among others.[15] Relivion MG is the device that most resembles Cefaly Dual; it is a trigeminal and occipital nerve stimulator that is placed around the head and held in place with a headband. This device was approved March 2021 by the FDA, and it is cleared for people aged 18 and older with a prescription from a doctor. Some of the side effects of this device are skin reactions, unpleasant sensation during treatment, pain and scalp reactions.

Cefaly Dual was the first FDA-approved trigeminal nerve stimulator to treat acute migraines. The Relivion MG is the only device that uses this same type of technology, but it has only been on the market since 2021 and requires a prescription. The approval of Cefaly came after the PREMICE trial, a randomized, controlled trial conducted by the Belgian Headache Society between the years 2009 and 2011.[16] In this study, more than 50% reduction of monthly migraines were recorded after the use of the Cefaly device 20 minutes daily for three months.[17] This proved the efficacy of Cefaly Dual as a preventative migraine treatment option in addition to an acute treatment option, making it the only device that offers both types of treatment.

Although there are many similarities between these devices and Cefaly Dual, the Cefaly device has some clear advantages and disadvantages against others on the market. Cefaly is the only device proven to prevent migraines, in addition to treat acute attacks.[17] It is the only device that is over the counter, which would make it more desirable for a patient that would not want to go to a physician to get treatment. The price is also on the lower side, costing $378 for the main device and $20 each pack of three electrodes; this price can also be lowered by joining a subscription.[18] However, this is the only device that is not covered by any insurance companies,

although payment plans can be arranged.[19] As a company, Cefaly has the biggest revenue of them all, with a revenue of $10.14M in 2021,[20] compared to the $5M made by Theranica (Nerivio)[21] and $5.5M made by electroCore (GammaCore).[22] A major disadvantage for Cefaly is that their patent only protects their specific method of electrode attachment via adhesive gel and stimulation of the trigeminal nerve, leaving the door open for companies like Relivion to create an extremely similar product to undercut Cefaly's market share.[23] This relatively weak IP causes concern for acquisition, despite the advantages of being first to market and over-the-counter.

V. Conclusion and Recommendation

Our biophysical model indicates a questionably low ratio of Aß to A∂ fiber activation, raising concern over the proposed gate control theory mechanism of action. Significant A∂ fiber activation was seen in the STN-M across all therapeutically reasonable stimulus ranges, indicating users would likely feel pain at the sites of stimulation. This provides further evidence for claims that a significant amount of users are unsatisfied with Cefaly. A growing market indicates increased market competition, and we determined development of similar devices such as the Relivion prove weak protection of Cefaly's intellectual property. The fact that this product is not covered by any insurance also makes the product less desirable than other options from a patient's perspective. Cefaly Dual is also only approved for patients 18 and older as opposed to other devices which are approved for younger ages, meaning a significant loss in the total portion of the market population. Based on these arguments, we do not recommend Johnson & Johnson acquire Cefaly Dual.

VI. Appendix

D_f = Fiber Diameter (μm)

$$\text{Node Diameter } (\mu m) = 0.01093 * D_f^2 + 0.1008 * D_f + 1.099$$

$$\text{Axon Diameter } (\mu m) = 0.02361 * D_f^2 + 0.3673 * D_f + 0.7122$$

$$\text{FLUT Segment Length } (\mu m) = -0.1652 * D_f^2 + 6.354 * D_f - 0.2862$$

$$\text{Internodal Spacing Length } (\mu m) = 81.08 * D_f + 37.84$$

$$\text{Number of Myelin Lamellae} = -0.4749 * D_f^2 + 16.85 * D_f - 0.7648$$

Equation 1: Interpolation Equations for A∂ Fibers

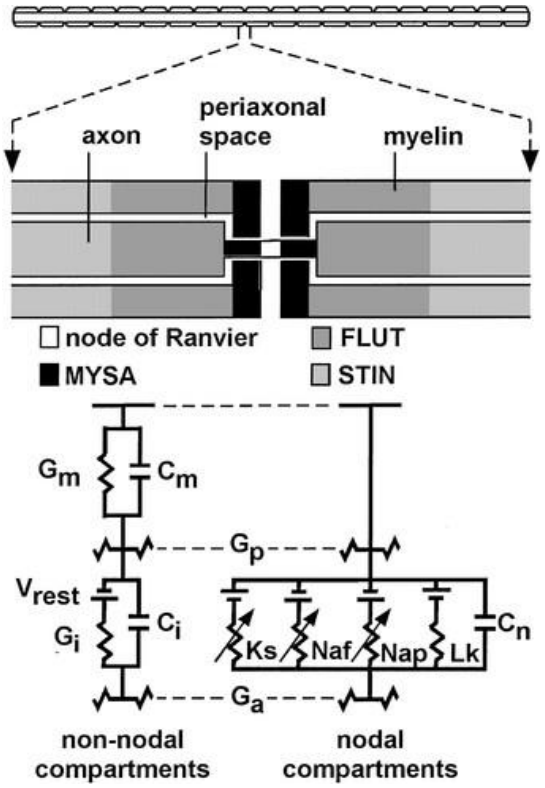

Figure 1: McIntyre-Richardson-Grill multi-compartment, double layer cable model of a mammalian axon[7]

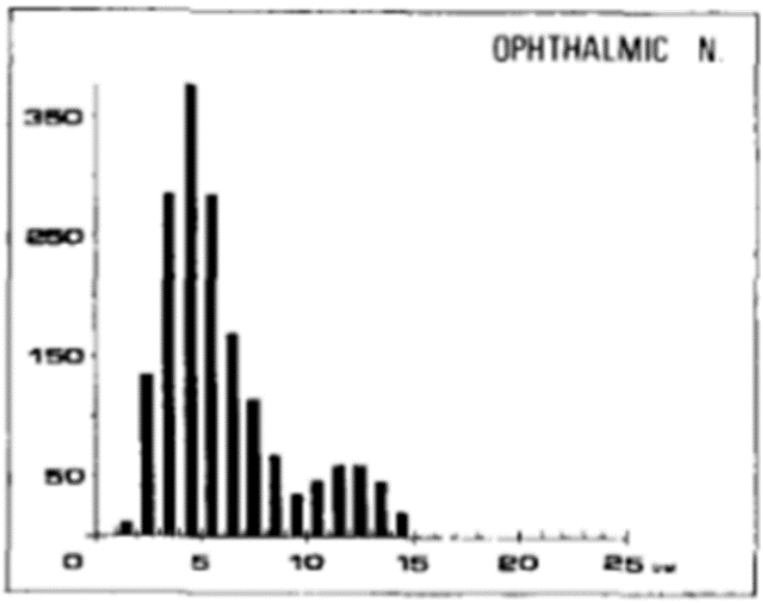

Figure 2: Histometric analysis density plot of fiber diameters found within the ophthalmic nerve, the root nerve of the SON and STN[2]

Parameter	#	Mean	SD
Location of lacrimal caruncle			
From facial midline	1	20.6	1.9
Emerging point of the STN			
From lacrimal caruncle	2	3.4	1.9
STN-M piercing the CS			
Horizontal	3	3.7	2.5
Vertical	4	0	1.8
STN-L piercing the CS			
Horizontal	5	1.8	3.8
Vertical	6	2.2	3.5
STN-M piercing the frontalis muscle			
Horizontal	7	9.2	3.8
Vertical	8	9.6	5.1
STN-L piercing the frontalis muscle			
Vertical	10	15.3	7.9
Horizontal	9	1.1	4.5

Detailed descriptions are provided in the text (see measurements section in the Materials and Methods) and Figure 2.

Measurement units are in millimeters.

#, parameter number; CS, corrugator supercilii muscle; STN, supratrochlear nerve; STN-M, medial branch of the STN; STN-L, lateral branch of the STN.

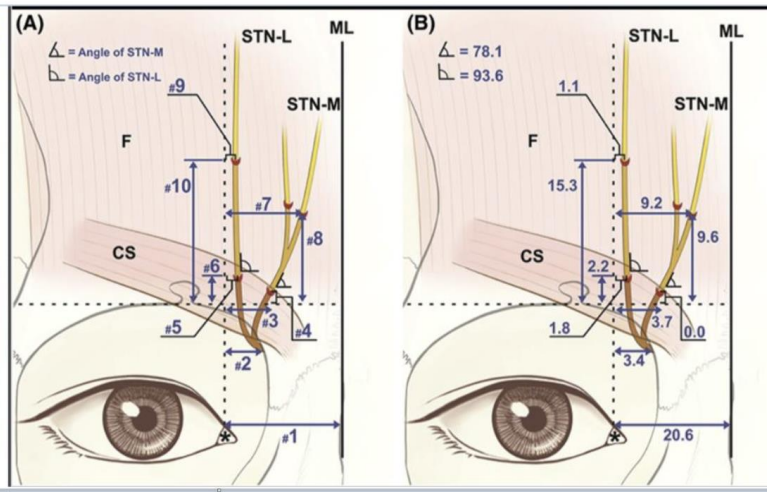

Figure 3: STN geometric values and schematic used to model STN-M and STN-L branches[9]

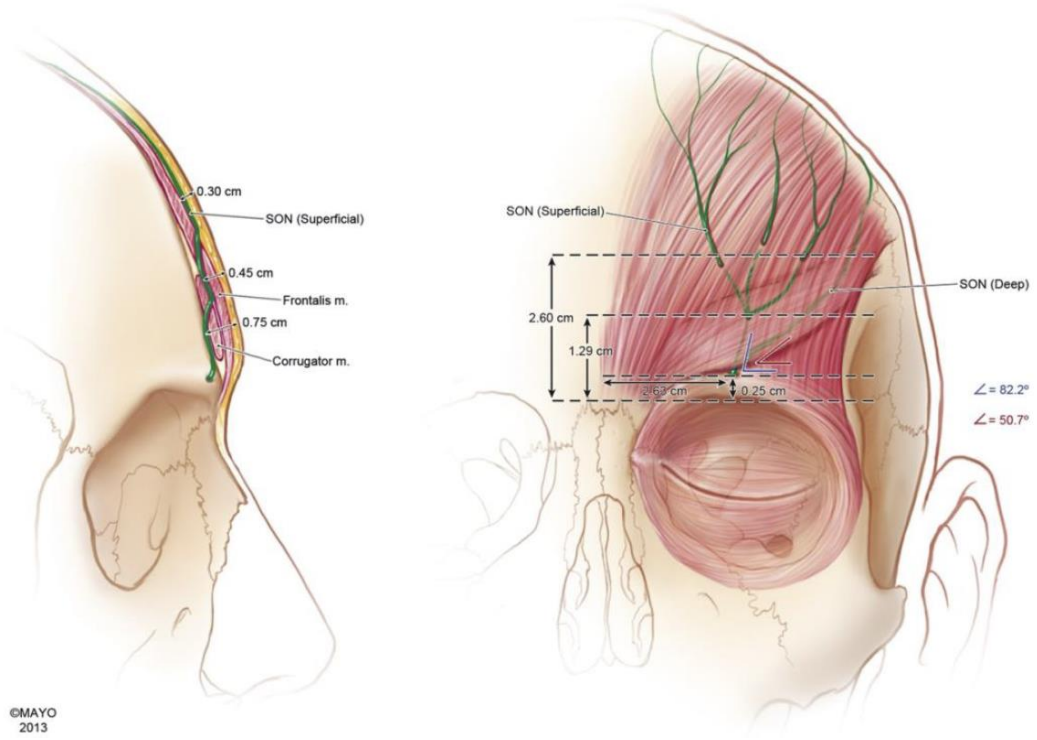

Figure 4: SON location averages obtained from sixteen cadaveric specimens used to model SON variations[10]

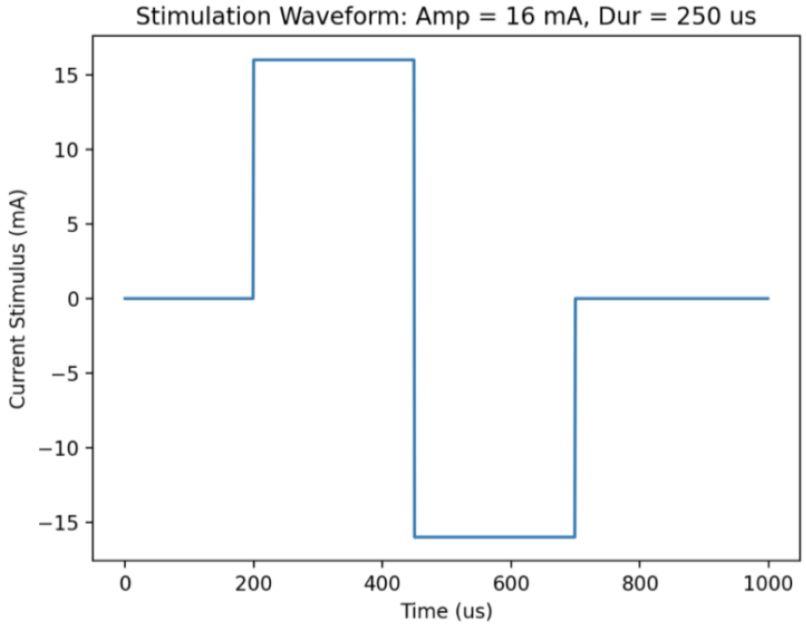

Figure 5: Stimulation waveform with amplitude of 16 mA and pulse duration of 250 us

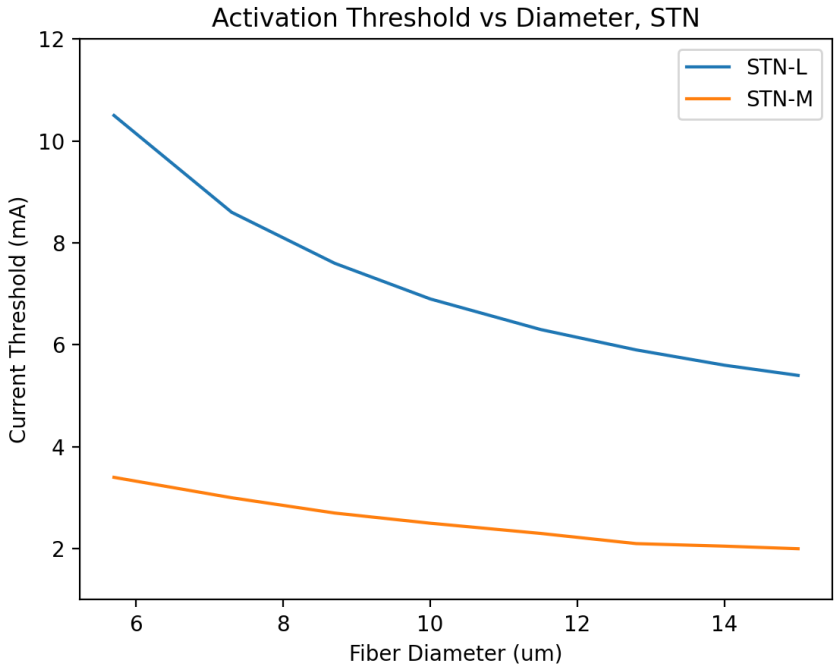

Figure 6: Activation threshold (mA) vs. fiber diameter (µm) of Aß fibers for STN-L and STN-M branches

Fiber Diameter (um)	STN-L Current Threshold (mA)	STN-M Current Threshold (mA)
5.7	10.5	3.4
7.3	8.6	3
8.7	7.6	2.7
10	6.9	2.5
11.5	6.3	2.3
12.8	5.9	2.1
14	5.6	2.1
15	5.4	2

Table 1: Activation threshold (mA) vs. fiber diameter (µm) of Aß fibers for STN-L and STN-M branches

SON Variations	Horizontal Distance from Midline (mm)
SON 1	19.26
SON 2	19.53
SON 3	20.07
SON 4	20.34

Table 2: Horizontal distances from midline of four SON variations

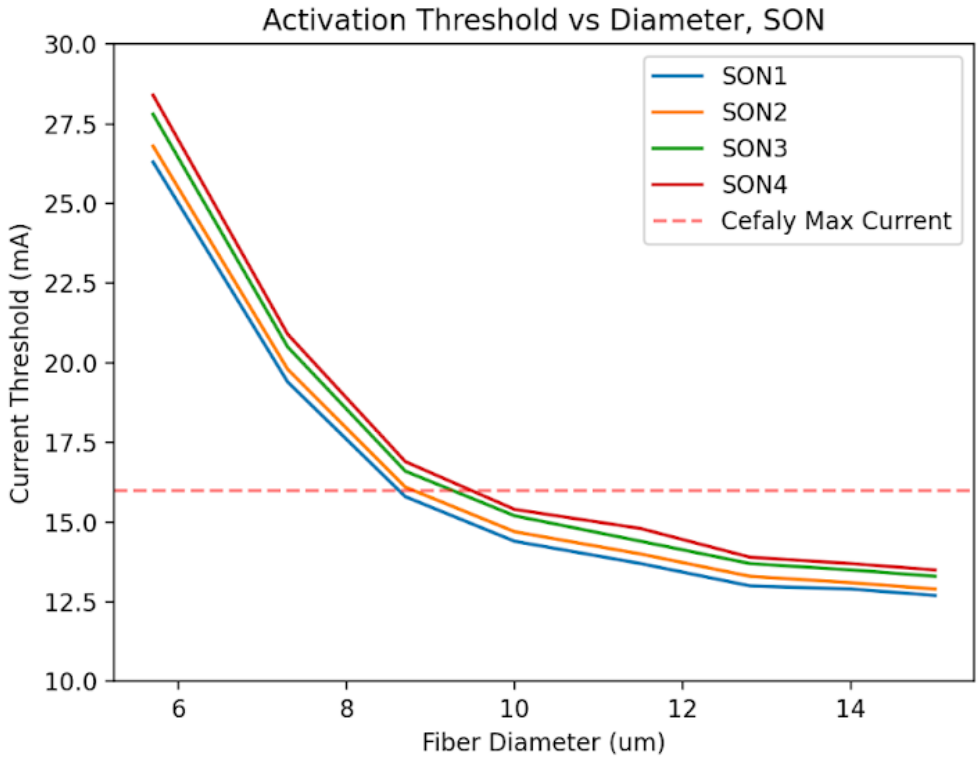

Figure 7: Activation threshold (mA) vs. fiber diameter (µm) of Aß fibers for four SON variations

Fiber Diameter (um)	SON1 Current Threshold (mA)	SON2 Current Threshold (mA)	SON3 Current Threshold (mA)	SON4 Current Threshold (mA)
5.7	26.3	26.8	27.8	28.4
7.3	19.4	19.8	20.5	20.9
8.7	15.8	16.1	16.6	16.9
10	14.4	14.7	15.2	15.4
11.5	13.7	14	14.4	14.8
12.8	13	13.3	13.7	13.9
14	12.9	13.1	13.5	13.7
15	12.7	12.9	13.3	13.5

Table 3: Activation threshold (mA) vs. fiber diameter (µm) of Aß fibers for four SON variations

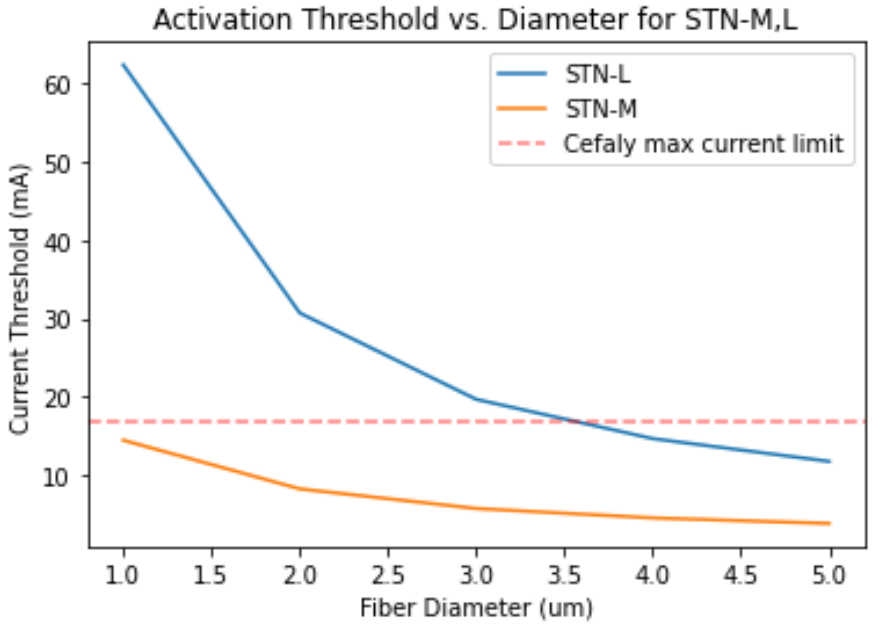

Figure 8: Activation threshold (mA) vs. fiber diameter (µm) of A∂ fibers for STN-L and STN-M branches

Fiber Diameter (um)	STN-L Current Threshold (mA)	STN-M Current Threshold (mA)
1	62.3	14.5
2	30.7	8.3
3	19.7	5.8
4	14.7	4.6
5	11.8	3.9

Table 4: Activation threshold (mA) vs. fiber diameter (μm) of A∂ fibers for STN-L and STN-M branches

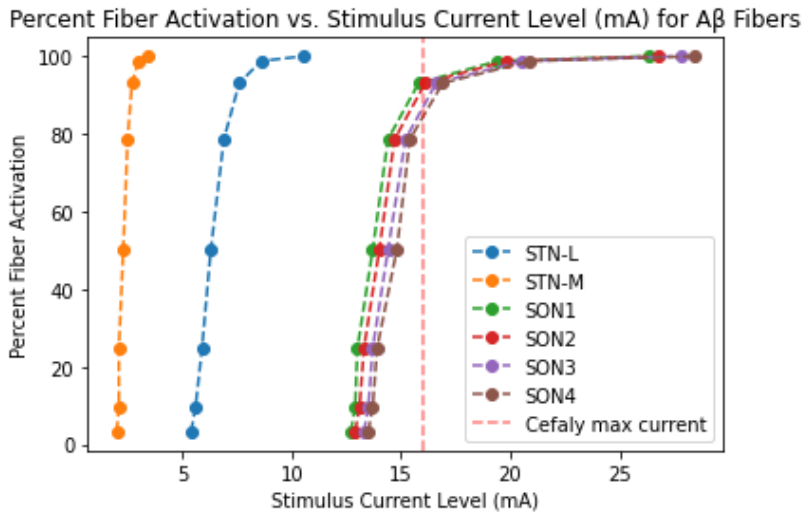

Figure 9: Percent fiber activation vs. stimulus current level for Aß fibers across all nerve branches

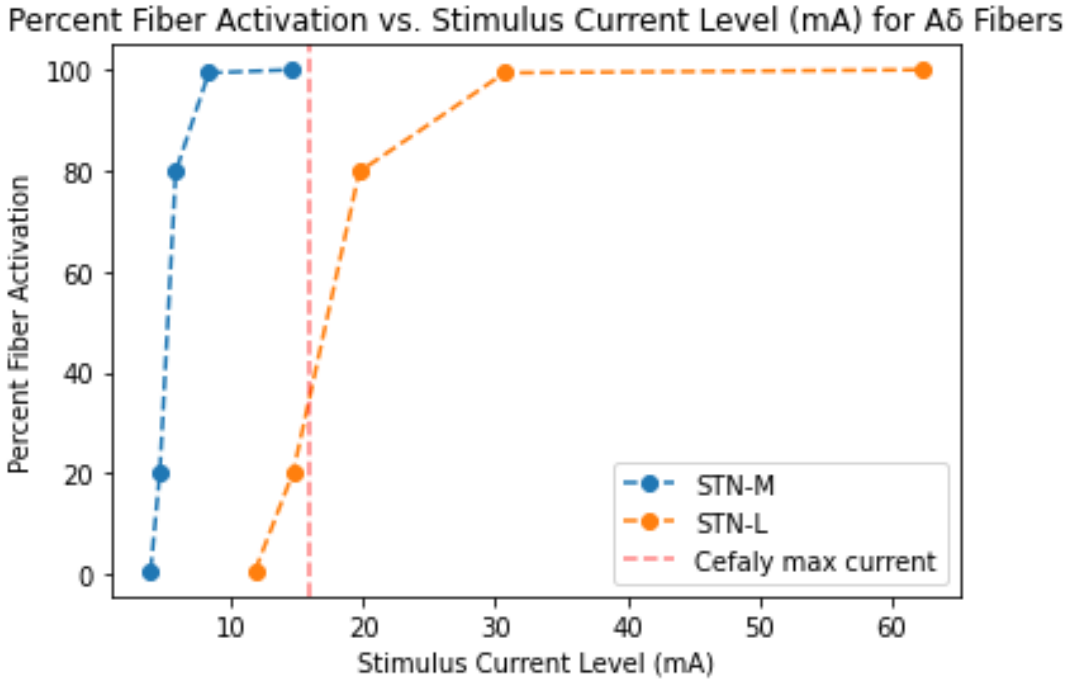

Figure 10: Percent fiber activation vs. stimulus current level for A∂ fibers across STN-M, STN-L branches (no activation in any SON)

Aβ Fiber Activation (%)						
Current (mA)	STN-L	STN-M	SON1	SON2	SON3	SON4
14.4	100	100	78.51	50	50	24.69
16	100	100	92.97	78.51	78.51	78.51
Aδ Fiber Activation (%)						
Current (mA)	STN-L	STN-M	SON1	SON2	SON3	SON4
14.4	99.38	0.62	0	0	0	0
16	20.23	100	0	0	0	0

Table 5: Aß and A∂ fiber activation (%) vs. stimulation current levels of interest across all branches

Total A beta Fiber Activation		
Branches	Current (mA)	
	14.4	16
STNs + SON1	278.51	292.97
STNs + SON2	250	278.51
STNs + SON3	250	278.51
STNs + SON4	224.69	278.51
Total A delta Fiber Activation		
Branches	Current (mA)	
	14.4	16
STNs + SON1	100	120.23
STNs + SON2	100	120.23
STNs + SON3	100	120.23
STNs + SON4	100	120.23
A beta / A delta Activation Ratios		
Branches	Current (mA)	
	14.4	16
STNs + SON1	2.7851	2.4367
STNs + SON2	2.5	2.3165
STNs + SON3	2.5	2.3165
STNs + SON4	2.2469	2.3165

Table 6: Total fiber activations and ratios for each branch combination

VII. References

1. *The true pain of migraine misconceptions: AMF*. American Migraine Foundation. (2022, March 8). Retrieved April 27, 2022, from https://americanmigrainefoundation.org/resource-library/the-true-pain-of-migraine-misconceptions/
2. Food and Drug Administration. (n.d.). *501(k) Correspondence to Cefaly*. Retrieved April 27, 2022, from https://www.accessdata.fda.gov/cdrh_docs/pdf20/K201895.pdf
3. Chou et al. "Acute migraine therapy with external trigeminal neurostimulation (ACME): A randomized control trial." *Cephalalgia.* Vol. 39, no. 1, 2019, pp. 3-14.
4. Kandel, Eric R., et al. "Principles of Neural Science." *McGraw Hill*, 2021.
5. Salkim, E; Shiraz, AN; Demosthenous, A. "Computational Study on Transcutaneous Frontal Nerve Stimulation: Simplification of Human Head Model." (Proceedings) COMSOL Conference. 2017, pp. 18-21

6. Salkim, E et al. "Impact of Neuroanatomical Variations and Electrode Orientation on Stimulus Current in a Device for Migraine: A Computational Study." *Journal of Neural Engineering.* Vol. 17, no. 1, 2019, p. 016006
7. McIntyre CC, Richardson AG, Grill WM. "Modeling the excitability of mammalian nerve fibers: influence of afterpotentials on the recovery cycle." *J Neurophysiology*. Vol. 87, 2002, pp. 995-1006.
8. Melzack, R., & Wall, P. D. (n.d.). *Pain mechanisms: A new theory - University of Pittsburgh*. Retrieved April 27, 2022, from http://pcpr.pitt.edu/wp-content/uploads/2018/01/Melzack-Wall.pdf
9. Gil, Young-Chun & Lee, et al. (2017). "Three-Dimensional Topography of the Supratrochlear Nerve With Reference to the Lacrimal Caruncle, and Its Danger Zone in Asians." *Dermatologic Surgery*. Vol. 43, no. 12, 2017, pp. 1458-1465.
10. Christenson, K et al. "Cutaneous Depth of the Supraorbital Nerve." *Dermatologic Surgery*. Vol. 40, no. 12, 2014, pp. 1342-1348.
11. *Migraines Overview*. UpToDate. (n.d.). Retrieved April 27, 2022, from https://www.uptodate.com/contents/migraines-in-adults-beyond-the-basics#H1
12. Samuelsson, O. (2021, September 29). *Market report predicts strong growth for Neuromodulation*. BioStock. Retrieved April 27, 2022, from https://www.biostock.se/en/2021/09/market-report-predicts-strong-growth-for-chordate-medicals-technology/
13. *Nerivio for the treatment of Migraine*. Medical Device Network. (2022, February 16). Retrieved April 27, 2022, from https://www.medicaldevice-network.com/projects/nerivio-treatment-migraine/
14. Theranica. (2021, April 12). *NERIVIO® wearable migraine therapeutic now eligible for insurance coverage through UpScript's telemedicine platform*. Retrieved April 27, 2022, from https://www.prnewswire.com/il/news-releases/nerivio-wearable-migraine-therapeutic-now-eligible-for-insurance-coverage-through-upscripts-telemedicine-platform-301266552.html
15. Kirsh, D. (2019, June 18). *11 innovative medical devices you need to know from 2018 - page 5 of 12*. Medical Design and Outsourcing. Retrieved April 27, 2022, from https://www.medicaldesignandoutsourcing.com/innovative-medical-devices-2018/5/
16. Naveed Saleh, M. D. (2022, January 18). *Cefaly neurostimulation: A new way to treat migraine attacks*. Verywell Health. Retrieved April 27, 2022, from https://www.verywellhealth.com/cefaly-migraine-prevention-and-treatment-4156863

17. Schoenen, J., Vandersmissen, B., Jeangette, S., Herroelen, L., Vandenheede, M., Gerard, P., & Magis, D. (2013). Prevention of migraine by supraorbital transcutaneous neurostimulation using the Cefaly® device (PREMICE): a multi-centre, randomized, sham-controlled trial. The Journal of Headache and Pain, 14(Suppl 1), P184. https://doi.org/10.1186/1129-2377-14-S1-P184
18. MediLexicon International. (n.d.). *Cefaly for Migraine Review: What to know*. Medical News Today. Retrieved April 27, 2022, from https://www.medicalnewstoday.com/articles/cefaly
19. GoodRx. (n.d.). *4 FDA-cleared devices that can treat your migraine*. GoodRx. Retrieved April 27, 2022, from https://www.goodrx.com/conditions/migraine/consumer-devices-for-migraine-treatment-and-prevention
20. *Cefaly technology company profile: Seraing, Liege, Belgium: Competitors, Financials & Contacts - Dun & Bradstreet*. Dun & Bradstreet - Accelerate Growth and Improve Business Performance. (n.d.). Retrieved April 27, 2022, from https://www.dnb.com/business-directory/company-profiles.cefaly_technology.883aeb6fd12587e22d014c601a6d82a9.html
21. *Theranica - Overview, News & Competitors*. ZoomInfo. (n.d.). Retrieved April 27, 2022, from https://www.zoominfo.com/c/theranica/375066175
22. BioSpace. (2022, March 10). *Electrocore announces fourth quarter and full year 2021 financial results*. BioSpace. Retrieved April 27, 2022, from https://www.biospace.com/article/releases/electrocore-announces-fourth-quarter-and-full-year-2021-financial-results/
23. *Patents assigned to Cefaly technology sprl - justia patents search*. Justia. (n.d.). Retrieved April 27, 2022, from https://patents.justia.com/assignee/cefaly-technology-sprl

VIII. Annex

Our code is public and can be accessed through the following link:

https://github.com/braden2447/BME-515-Project